Biochemical Pharmacology 80 (2010) 884–894

Contents lists available at ScienceDirect

Biochemical Pharmacology

journal homepage: www.elsevier.com/locate/biochempharm

Olesoxime prevents microtubule-targeting drug neurotoxicity: Selective preservation of EB comets in differentiated neuronal cells

Amandine Rovini [a], Manon Carré [a,*], Thierry Bordet [b,1], Rebecca M. Pruss [b,1], Diane Braguer [a]

[a] INSERM UMR911, Centre de Recherche en Oncologie biologique et Oncopharmacologie, Aix-Marseille Université, Faculté de Pharmacie, 27 Boulevard Jean Moulin, 13385 Marseille Cedex 5, France
[b] Trophos, Parc Scientifique de Luminy, Luminy Biotech Entreprises, Case 931, 13288 Marseille Cedex 9, France

ARTICLE INFO

Article history:
Received 16 December 2009
Accepted 15 April 2010

Keywords:
Neuroprotection
Microtubule
EB proteins
Mitochondria
Taxanes
Vinca alkaloids

ABSTRACT

Microtubule-targeting agents (MTAs), anticancer drugs widely used in the clinic, often induce peripheral neuropathy, a main dose-limiting side effect. The mechanism for this neurotoxicity remains poorly understood and there are still no approved therapies for neuropathies triggered by MTAs. Olesoxime (cholest-4-en-3-one, oxime; TRO19622) has shown marked neuroprotective properties in animals treated with paclitaxel and vincristine. The purpose of this study was to investigate its mechanism of neuroprotection against MTA neurotoxicity by using rat and human differentiated neuronal cells. We first showed that olesoxime prevented neurite shrinkage induced by MTAs in differentiated PC-12 and SK-N-SH neuroblastoma cell lines by up to 90%. This neuroprotective effect was correlated with enhanced EB1 accumulation at microtubule plus-ends, increased growth cone microtubule growing rate (20%) and decreased microtubule attenuation duration (54%). The effects of olesoxime on EB comets were specific for differentiated neuronal cells and were not seen either in proliferating neuroblastoma cells, glioblastoma cells or primary endothelial cells. Importantly, olesoxime did not alter MTA cytotoxic properties in a wide range of MTA-sensitive tumor cells, a prerequisite for future clinical application. Finally, olesoxime also counteracted MTA inhibition of microtubule-dependent mitochondria trafficking. These results provide additional insight into the neuroprotective properties of olesoxime, highlighting a role for microtubule dynamics in preservation of neurite architecture and axoplasmic transport, which are both disturbed by MTAs. The neuron-specific protective properties of olesoxime support its further development to treat MTA-induced neuropathy.

1. Introduction

Chemotherapy-induced peripheral neuropathy (CIPN) is the main dose-limiting side effect of commonly used microtubule-targeting agents (MTAs), including taxanes and Vinca alkaloids, but also newer agents such as epothilones [1–3]. Typically, the clinical presentation reflects an axonal peripheral neuropathy with glove-and-stocking distribution sensory loss, combined with features suggestive of nerve hyperexcitability including paresthesia, dysesthesia, and pain. Most of the time, peripheral neuropathy reverses if the treatment is stopped; however, in some cases, recovery from symptoms is incomplete and a long period of regeneration is required to restore function [4]. Although several neuroprotective agents have been proposed (recently reviewed in [5]), to date, there are no approved therapies for prevention or treatment of neuropathies triggered by MTA chemotherapy [2,3,6].

Mechanisms underlying MTA-induced neurotoxicity are still poorly understood. Using rat models, it was demonstrated that whereas low doses of paclitaxel does not lead to massive axonal degeneration [7,8] as initially thought, it causes partial terminal arbor degeneration of myelinated and unmyelinated nerve fibers in the epidermis [9]. In neuronal cultures, paclitaxel significantly reduced dendritic branching and length of neurites [10,11]. This suggests that paclitaxel may disrupt specific microtubule function in nerve processes. Microtubule dynamics, which is the switch between phases of growth and shortening, is of particular importance for the development and maintenance of nerve processes [12]. It is highly controlled by microtubule plus-end tracking proteins (+TIPs), an evolutionary conserved family of proteins that specifically form comet-like accumulation at the ends of growing microtubules. End binding protein-1 (EB1) and -3 (EB3), two major members of the +TIPs family, are particularly involved in axonal growth and elongation, as well as in neurotransmitter receptor positioning in terminally differentiated neurons [13–15].

* Corresponding author at: INSERM UMR911 (CRO2), Faculté de Pharmacie, 27 Bd Jean Moulin, 13385 Marseille Cedex 05, France. Tel.: +33 491835626; fax: +33 491835506.
E-mail addresses: arovini@pharmacie.univ-mrs.fr (A. Rovini), manon.carre@pharmacie.univ-mrs.fr (M. Carré), tbordet@trophos.com (T. Bordet), rpruss@trophos.com (R.M. Pruss), diane.braguer@univmed.fr (D. Braguer).
[1] These authors are employees of Trophos.

0006-2952/$ – see front matter © 2010 Elsevier Inc. All rights reserved.
doi:10.1016/j.bcp.2010.04.018

Paclitaxel treatment decreased the number of detectable EB3-GFP comet tails in cultured Aplysia neurons, altering the dynamic properties of neuronal microtubules as demonstrated by impaired vesicles and mitochondrial transport [16]. Taken together, these results led to the emerging hypothesis that defects in microtubule dynamics and malfunction of +TIPs are closely related to the onset of CIPN and possibly other neurological disorders [17].

Olesoxime (cholest-4-en-3-one, oxime; TRO19622) is a small cholesterol-like compound with marked neuroprotective and neuroregenerative properties. In vitro, olesoxime favors neurite outgrowth and branching of spinal motor neurons, and maintains their survival as efficiently as a cocktail of three neurotrophic factors [18]. In vivo, olesoxime significantly reduced axonal degeneration and accelerated recovery of motor nerve conduction in a model of peripheral neuropathy induced by crushing the sciatic nerve [19]. Similarly, daily oral administration of olesoxime improved motor nerve conduction impaired in streptozotocin-induced diabetic rats, reversing neuropathic pain behavior [19]. Olesoxime also reversed tactile allodynia in vincristine-induced CIPN while it had no analgesic activity per se [20]. In paclitaxel-treated rats, olesoxime was recently shown to not only reverse mechano-allodynia and mechano-hyperalgesia in both preventive and prophylactic treatment paradigms but also to significantly reduce paclitaxel-induced sensory terminal arbor degeneration [20]. Altogether these results suggest that, beyond its acute antinociceptive effects, olesoxime displayed neuroprotective and/or regenerative properties that could counteract MTA-induced neurotoxicity.

The aim of this study was to further decipher olesoxime's mechanism of neuroprotection in cellular models of chemotherapy-induced neurotoxicity. Here, we show that olesoxime potently protected both rat and human neuron-like cells against MTA-induced neurite shrinkage. These neuroprotective properties were correlated with prevention of EB1 and EB3 delocalization from microtubule plus-ends and with inhibition of microtubule-governed mitochondria trafficking alteration induced by MTAs, suggestive of a preserved microtubule dynamics. Importantly, olesoxime counteracted MTA activity only in differentiated neuronal cells, since it maintained the anticancer efficacy of MTAs in proliferating human tumor cells, including neuroblastoma cells. Olesoxime selectivity could be related to its ability to increase EB1 comet length and microtubule dynamics only in differentiated neuronal cells. These results identify maintenance of neuronal microtubule dynamics and organelle trafficking as relevant endpoints for evaluating new neuroprotective therapeutics.

2. Material and methods

2.1. Cell culture and differentiation

Human umbilical vein endothelial cells (HUVEC) were obtained from the Cell Culture Laboratory in the Hôpital de la Conception (Assistance Publique, Hôpitaux de Marseille, Marseille, France); human lung carcinoma (A549), breast adenocarcinoma (MCF-7), neuroblastoma (SHEP and SK-N-SH) and glioblastoma (U87) were purchased at the ATCC. These proliferating cells were routinely maintained as we previously described [21,22]. Rat pheochromocytoma PC-12 cells were grown in RPMI-1640 medium supplemented by 5% fetal bovine serum, 10% horse serum, 1% L-glutamine, 1% penicillin and streptomycin (BioWhittaker, Verviers, Belgium).

For differentiation, SK-N-SH cells were seeded at 7000 cells/cm^2 on type I collagen coated plates and exposed to 6 μg/mL all-trans retinoic acid (ATRA; Sigma) for 96 h in complete RPMI medium. To be differentiated, PC-12 cells were seeded at 3000 cells/cm^2 on type I collagen (30 μg/mL; Sigma) coated plates and incubated for 96 h with 50 ng/mL β-nerve growth factor (NGF; Sigma) in complete RPMI medium containing 1% horse serum.

2.2. Drugs

Stock solution of paclitaxel (Alexis, Lausen, Switzerland) was prepared in DMSO while vincristine (Lilly, Strasbourg, France) and vinorelbine (Sigma) were prepared in aqueous solutions; the three MTAs were conserved at −20 °C. Stock solution of olesoxime in DMSO (Trophos SA, Marseille, France) was conserved at 4 °C. Because 10 μM olesoxime was toxic to neuronal cells in culture (personal data), 3 μM was considered the optimal concentration to combine to MTAs, in agreement with previous results obtained in vitro with rat motor neurons [18]. For experiments in living cells, drugs were freshly diluted in culture medium. Final concentration of DMSO in culture medium (drug-treated cells or vehicle conditions) was limited to 0.2%.

2.3. Neurite length measurement

PC-12 and SK-N-SH cells were seeded in 12-well plates to be differentiated during 96 h. Then, cells were exposed to MTAs alone or combined with olesoxime. After a 24-h treatment, cells were fixed with 3.7% formaldehyde for 10 min at 37 °C. Images were acquired with a Leica DM-IRBE microscope coupled with a digital camera (CCD camera cool snapFX), and neurite length was measured by using Metamorph® software (Princeton Instrument). At least three independent experiments were performed, and up to 1500 cells were analysed per condition. Data were expressed as mean ± SEM and statistical analysis was performed using Student's *t*-test. Significant difference between two conditions was retained for $p < 0.05$.

2.4. Cytotoxicity tests

Human tumor cells were seeded in 96-well plates to be treated during 72 h with MTAs alone or combined with olesoxime. Cell death was measured by using the colorimetric 3-(4,5-dimethylthiazol-2-yl)-2,5-diphenyltetrazolium bromide (MTT) assay (Sigma), as we described [23]. Absorbance was measured at 450 nm with a Multiskan (Ascent) plate reader. The computer program Calcusyn software (Biosoft) was used to draw median effect plots, i.e. log (dose) *vs* log (fraction of cells affected/fraction not affected), according to the Chou and Talalay's method and as we previously described [24]. X-intercept of these lines corresponds to log (IC_{50}). The same procedure was used to evaluate death of differentiated neuronal cells treated for 24 h with drugs. Three independent experiments were performed in quadruplicates and data were expressed as mean ± SEM.

For apoptosis detection, DNA was stained with 0.25 μg/mL 4′,6-diamidino-2-phenylindole (DAPI; Sigma), and the percentages of cells in interphase, mitosis and apoptosis were quantified. Apoptotic cells were defined by the condensation of nuclear chromatin and nuclear fragmentation [24].

2.5. Determination of intracellular vincristine concentration

Differentiated SK-N-SH neuronal cells were incubated with 100 nM vincristine alone or combined with 3 μM olesoxime for 24 h. Then, cells were sonicated in PBS and, after centrifugation [25], vincristine concentration in supernatants has been measured by LC/MS/MS as described in Guilhaumou et al. [26].

2.6. Immunofluorescence staining and comet length measurement

Human cancer cells were grown on Labtek chamber slides (Nunc, Roskilde, Denmark) and incubated with drugs for 24 h.

Then, cells were fixed and permeabilized as we previously described [24], and incubated with FITC-conjugated α-tubulin antibodies (clone DM1A; Sigma). Differentiated neuronal cells were incubated with drugs for 6–24 h, before being incubated with antibodies directed against EB1 (clone 5; BD Transduction Laboratories, Franklin Lakes, NJ) [27] and with TRITC-conjugated secondary antibodies (Jackson Immunosearch, West Grove, PA). Cells were observed using a Leica DM-IRBE microscope coupled with a digital camera driven by Metamorph® software (Princeton Instrument). EB comet length was measured by using Metamorph® software. At least three independent experiments were performed, and up to 180 comets were analyzed per condition. Data were expressed as mean ± SEM and statistical analysis was performed using Student's *t*-test. Significant difference between two conditions was retained for $p < 0.05$.

2.7. Western blotting

The protein content from whole cell lysates was determined according to the Bradford method, using Bio-Rad Protein Assay dye reagent (Bio-Rad Laboratories, France). Equal amounts of proteins (62.5 mM Tris pH 6.8, 0.5% SDS, 5% mercapto-ethanol, 10% glycerol) were separated by SDS-PAGE and electrotransferred onto a nitrocellulose membrane. Primary antibodies used were directed against EB1 (Cell signaling, Beverly, MA), α-tubulin (Sigma) and NSE (Zymed, San Francisco, CA). Peroxydase-conjugated goat anti-mouse antibodies were used as secondary antibodies (Jackson Immunoresearch, Baltimore, MD), and visualization was finally accomplished using a chemiluminescence detection kit (Millipore).

2.8. Time-lapse microscopy of microtubule plus-ends

To analyze microtubule plus-end dynamics, PC-12 cells were transfected with a plasmid coding for green fluorescent protein EB1-GFP [28]. Briefly, PC-12 cells (2×10^6) were resuspended in 100 μL of the specific electroporation V buffer (Amaxa, Walkersville, MD), and 4 μg of plasmid DNA were added to the cell suspension. The mixture was subjected to nucleofection (Nucleofector, Amaxa) and cells were immediately seeded on type I collagen coated glass coverslips in 6-well plates for differentiation. Then, cells were incubated for 24 h with 100 nM vincristine, 3 μM olesoxime, or both. To measure microtubule dynamics, cells were placed in a double coverslip chamber maintained at 37 °C, in RPMI culture medium supplemented with 0.1 mg/mL ascorbic acid (Aguettant, Lyon, France) as we previously described [29]. Time-lapse acquisitions were done on a Nikon TE 2000 fluorescence microscope. 31 images per cell were acquired at 2-s intervals using a digital camera (Ropper Scientific CoolSnap HQ). Positions of EB1 comets with time were then tracked by using Metamorph® software. Changes in length ≥0.2 μm were considered as growth events, while changes in length <0.2 μm were considered to be phases of attenuated dynamics or pause. Three independent experiments were performed, and more than 110 microtubules were analyzed for each experimental condition. Data were expressed as mean ± SEM. Statistical analysis was performed using Student's *t*-test; significant difference between two conditions was retained for $p < 0.05$. Kymographs were also built using Metamorph® software and, for quantitative analysis, the slope of the line was used to calculate the velocity of EB1 comets.

2.9. Time-lapse microscopy of mitochondria

SK-N-SH cells were seeded on type I collagen coated glass coverslips in 6-well plates to be differentiated and incubated for 24 h with 100 nM vincristine, 3 μM olesoxime, or both. To measure mitochondria velocity, cells were incubated with 25 μg/mL MitoTracker Red CMX-Ros (Molecular Probes) at 37 °C during 20 min. Then, videomicroscopy was performed as described for microtubule dynamics measurement. Three independent experiments were performed and at least 30 mitochondria were analyzed for each experimental condition. Data were expressed as mean ± SEM. Statistical analysis was performed using Student's *t*-test; significant difference between two conditions was retained for $p < 0.05$.

3. Results

3.1. Olesoxime inhibited MTA-induced neurite shrinkage in human and rat neuron-like cell lines

Because the neuroprotective effects of olesoxime have been demonstrated in vitro using primary rat motor neurons and in vivo in rats treated with MTAs, studies were performed using rat differentiated PC-12 cells and then extended to human differentiated SK-N-SH cells. Cell differentiation was confirmed by cellular quiescence and formation of long neurite outgrowths and further assayed in PC-12 cells by the expression of neuron-specific enolase (NSE) (Supplementary Fig. 1A and B). We first verified, by DAPI staining, that olesoxime (1–3 μM) did not display any cytotoxic effect in differentiated neuronal cells (Supplementary Fig. 2). Then, neurotoxicity of MTAs (24-h exposure) was characterized by measuring neurite length in the two cell lines. In differentiated PC-12 cells, vincristine induced a concentration-dependent decrease in mean neurite length from 19 ± 2% to 79 ± 3% with concentrations ranging from 20 to 100 nM ($p < 0.01$). Similarly, vincristine decreased neurite outgrowth in differentiated SK-N-SH cells up to 63 ± 3% at 200 nM ($p < 0.01$; Fig. 1A). Sensitivity of both neuronal cell lines to MTAs was confirmed with paclitaxel. Indeed, neurite length decreased 37 ± 7% and 78 ± 7% in differentiated SK-N-SH and PC-12 cells, with concentrations of 50 nM or 20 nM paclitaxel respectively (Fig. 1B and C). The effects of vincristine and paclitaxel on neurite outgrowth were not associated with apoptosis triggering (Supplementary Fig. 2), indicating that MTA-induced neurotoxicity is characterized by a loss of neuronal phenotype without cell death.

When simultaneously combined with vincristine (100 and 200 nM), olesoxime prevented neurite shrinkage in differentiated SK-N-SH cells in a concentration-dependent manner (Fig. 1B). While 1 μM olesoxime was not significantly effective, 2 μM was able to partially maintain neurite length in vincristine-treated cells ($p < 0.05$). Neurite rescue reached 60% with 3 μM olesoxime (Fig. 1B). 3 μM olesoxime also reduced neurite loss induced by 50 nM paclitaxel in differentiated SK-N-SH cells from 56 ± 2% to 44 ± 4% ($p < 0.05$; Fig. 1B). The neuroprotective potential of 3 μM olesoxime was confirmed in differentiated rat PC-12 cells where it rescued neurite length up to 90% when combined with either 50 nM vincristine ($p < 0.05$) or 20 nM paclitaxel ($p < 0.01$; Fig. 1C). By contrast, in the absence of MTAs, 24 hr treatment of differentiated PC-12 or SK-N-SH cells with olesoxime (1–3 μM) had no measurable effect on neurites (Fig. 1B and C). Interestingly, it is noteworthy that the intracellular concentration of vincristine in differentiated neuronal cells (580 ± 61 nM) was not decreased by its combination with olesoxime (700 ± 5 nM). Thus, the neuroprotective properties of olesoxime were not due to a decrease in vincristine accumulation.

3.2. Olesoxime did not interfere with MTA efficacy in tumor cells

To ensure that olesoxime does not preclude MTA cytotoxic properties, 3 μM olesoxime was evaluated in combination with paclitaxel or Vinca alkaloids in different human cancer cell lines, in agreement with their clinical use (Fig. 2). First, we ensured that olesoxime (1–3 μM) was not cytotoxic in lung cancer A549, breast cancer MCF-7 and neuroblastoma SHEP cells, as shown by MTT assay (Supplementary Table 1) and DAPI staining (Supplementary

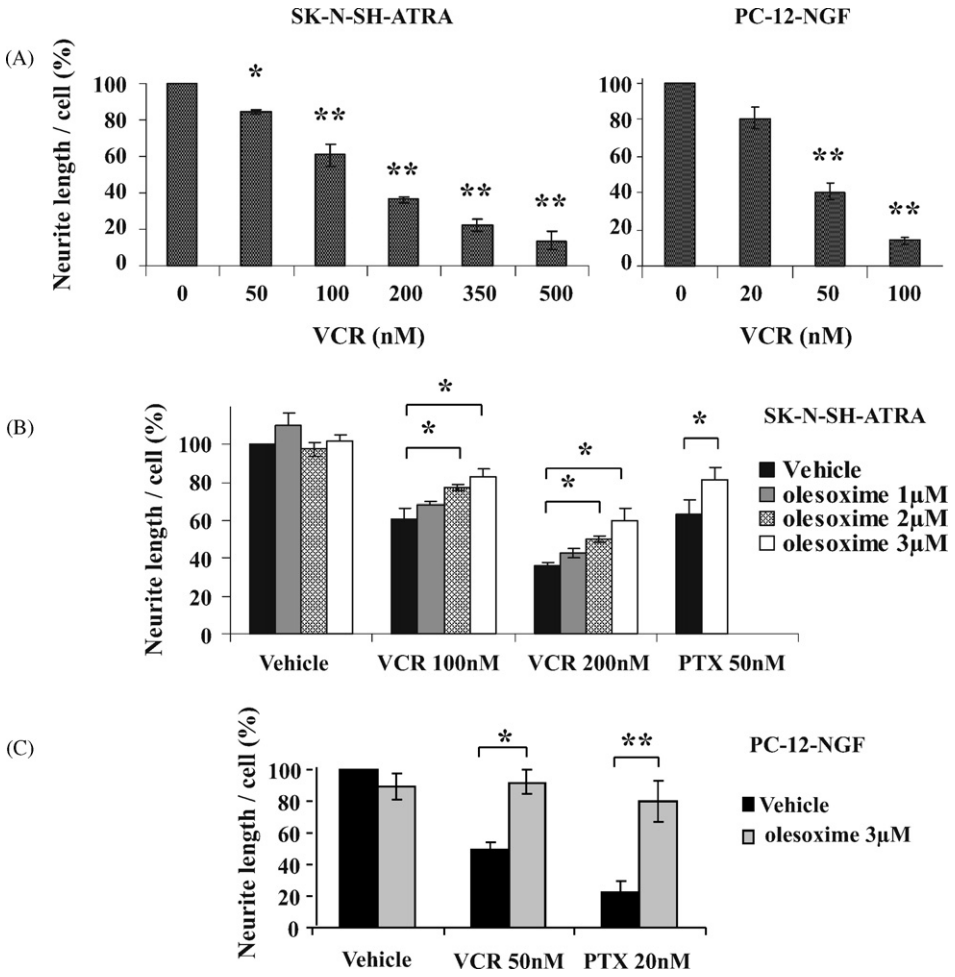

Fig. 1. Olesoxime prevented MTA-induced neurite shrinkage in differentiated neuronal cell lines. (A) Neurite length measurements after a 24-h treatment with increasing concentrations of vincristine (VCR) in differentiated SK-N-SH (SK-N-SH-ATRA) or PC-12 (PC-12-NGF) cells. (B) Neurite length measurements in differentiated SK-N-SH cells exposed for 24 hr to increasing concentrations of olesoxime, 100 and 200 nM vincristine, 50 nM paclitaxel (PTX) and their combination. (C) Same analysis in differentiated PC-12 cells treated with 3 μM olesoxime, 50 nM vincristine or 20 nM paclitaxel, and their combination (*$p < 0.05$; **$p < 0.01$; Student's *t*-test).

Fig. 3A). Similarly, we verified that olesoxime did neither modify mitosis progression nor survival in non-malignant cells, *i.e.* human epithelial HaCaT and endothelial HUVEC cells (Supplementary Fig. 3B and C, supplementary Tables 2 and 3).

Then, in A549 cells treated with vinorelbine or paclitaxel, SHEP and SK-N-SH cells treated with paclitaxel or vincristine, and MCF-7 cells treated with paclitaxel, we showed that there was no significant difference in the cytotoxic efficacy of any of these MTAs in the presence or absence of olesoxime (Fig. 2A–C and data not shown) ($p > 0.05$). The similar *x*-intercept of median effect plots, and their general overlapping, also confirmed that MTA cytotoxic activity was not disturbed by olesoxime (Fig. 2A–C). Accordingly, quantification of mitotic nuclei by immunofluorescence showed that 3 μM olesoxime did not modify the mitotic block induced by paclitaxel (Table 1) or vinorelbine (data not shown) in A549, MCF-7 and SHEP cancer cells ($p > 0.05$). Altogether, our results indicate that olesoxime leads to a significant decrease in the neurotoxic effects of both taxanes and Vinca alkaloids without affecting their cytotoxic properties in human tumor cells, including proliferating neuroblastoma cells.

3.3. Olesoxime increased EB1 comet length and microtubule dynamics in neuronal cells

To further explore the mechanism of action to maintain neurite outgrowth, we evaluated the effects of olesoxime on microtubule dynamics in neuronal cells in the absence or presence of MTAs. Prior to these experiments, we confirmed that olesoxime had no effect on global microtubule cytoskeleton architecture (data not shown). Then, we examined the intracellular localization of EB1, a +TIP that ensures microtubule growth. In control differentiated SK-N-SH cells, EB1 displayed the expected comet-like distribution (Fig. 3A), with a mean length of 0.64 ± 0.02 μm (Table 2). Interestingly, a 6-h treatment with 3 μM olesoxime significantly increased comet length up to 0.85 ± 0.02 μm ($p < 0.01$), indicating that olesoxime is able to enhance EB1 accumulation at microtubule plus-ends in differentiated neuronal cells. In sharp contrast, EB1 comet length was not increased by olesoxime treatment in proliferating neuroblastoma SK-N-SH cells ($p > 0.05$; Table 2). Olesoxime selective triggering of EB1 accumulation in differentiated neuronal cells was further supported by its lack of effect on EB1 comet length in human glioblastoma U87 cells or primary human endothelial HUVECs (Table 2).

To evaluate whether the effect of olesoxime on EB1 comet length affected microtubule dynamics, we used live imaging fluorescence microscopy in differentiated PC-12 cells transfected with EB1-GFP to track microtubule plus-ends position in growth cones (see movie 1). Treatment for 24 h with 3 μM olesoxime promoted microtubule growing events (Table 3). Indeed, we determined that olesoxime increased by 24% the number of dynamic microtubules that spent all their time growing. Quantitative analysis of EB1 comet tracks showed that olesoxime

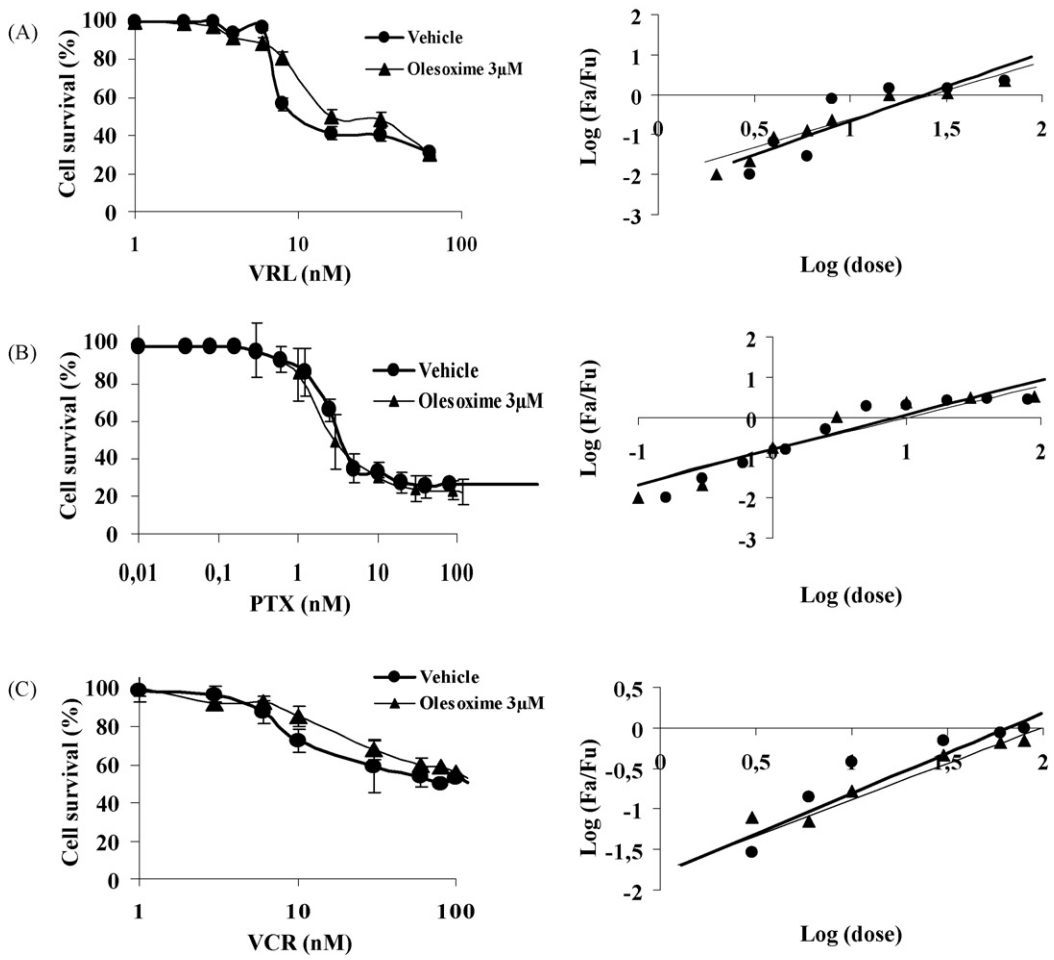

Fig. 2. Olesoxime did not reduce MTA cytotoxicity for proliferating cancer cells. Cytotoxicity of vinorelbine (VRL), paclitaxel (PTX) and vincristine (VCR) alone or in combination with 3 μM olesoxime, for 72 h, in (A) human lung cancer A549 cells, (B) human neuroblastoma SHEP cells and (C) human neuroblastoma SK-N-SH cells. Left graphs are dose-effect curves, and right graphs are median effect plots where Fa is the fraction of cells affected (cell death) and Fu the fraction not affected (cell survival).

increased microtubule growth rate by 20% ($p < 0.05$; Table 3). This effect has been confirmed by analysing kymographs, which revealed a 28% increase in EB1 comet velocity in olesoxime-treated neuronal cells, as illustrated in Fig. 3B. In parallel, olesoxime increased microtubule time growing by 4% ($p < 0.01$) and decreased by 54% their time pausing ($p < 0.01$; Table 3). These results showed that olesoxime increased microtubule dynamics in neurite outgrowths, which is likely related to its ability to enhance EB proteins localization at growing ends of microtubules in differentiated neuronal cells.

3.4. Olesoxime protected differentiated neuronal cells from MTA-induced EB comet disruption

We then studied the effect of MTAs on EB protein localization in differentiated neuronal SK-N-SH cells. Both paclitaxel (50 nM) and vincristine (100 nM) had a common profound effect on EB1 and EB3 distribution. Instead of its usual punctuate comet-like appearance, EB1 was displaced from microtubules to the cytosol, as indicated by the diffuse fluorescent signal observed after a short exposure (6 h) to MTAs (Fig. 4A). Similar results were also observed after a 24-h treatment (Supplementary Fig. 3). Furthermore, we found that EB3, another member of the EB family required for neuritogenesis, was also displaced from microtubules to cytosol by MTAs in differentiated SK-N-SH cells (data not shown). Thus, EB comet disruption, generally associated with microtubule dynamics perturbation, is a key event in both vincristine- and paclitaxel-induced neurotoxicity.

We then evaluated the impact of olesoxime on EB1 distribution in differentiated SK-N-SH cells treated with MTAs. Interestingly, 3 μM olesoxime prevented both vincristine- and paclitaxel-induced EB1 delocalization measured after 6 h (Fig. 4B), and this effect was maintained for up to 24 h (Supplementary Fig. 3). In addition, 2 μM olesoxime – which also displayed neuroprotective properties against MTA-induced neurite shrinkage – was able to maintain EB1 localization under MTA treatment, while 1 μM olesoxime – which did not prevent MTA-induced neurite shrinkage – did not counteract MTA effects on microtubule plus-ends (Supplementary Fig. 4). It is noteworthy that EB1 expression level was not modified either by MTAs or olesoxime treatment (Fig. 4C), confirming that major modifications in EB1 staining resulted from its spatial rearrangement. Moreover, as for EB1, EB3 localization at microtubule plus-ends was preserved when cells were simultaneously exposed to MTAs and olesoxime (data not shown),

Table 1
Olesoxime did not modify the mitotic block induced by MTAs. Percentage in mitosis ± SEM in A549, MCF-7 and SHEP cancer cells exposed for 24 h to paclitaxel 4 nM alone and combined with olesoxime 3 μM.

	A549	MCF-7	SHEP
PTX 4 nM	24 ± 7	31 ± 7	14 ± 3
PTX 4 nM + olesoxime 3 μM	23 ± 6 NS	28 ± 4 NS	12 ± 3 NS

NS, $p > 0.05$.

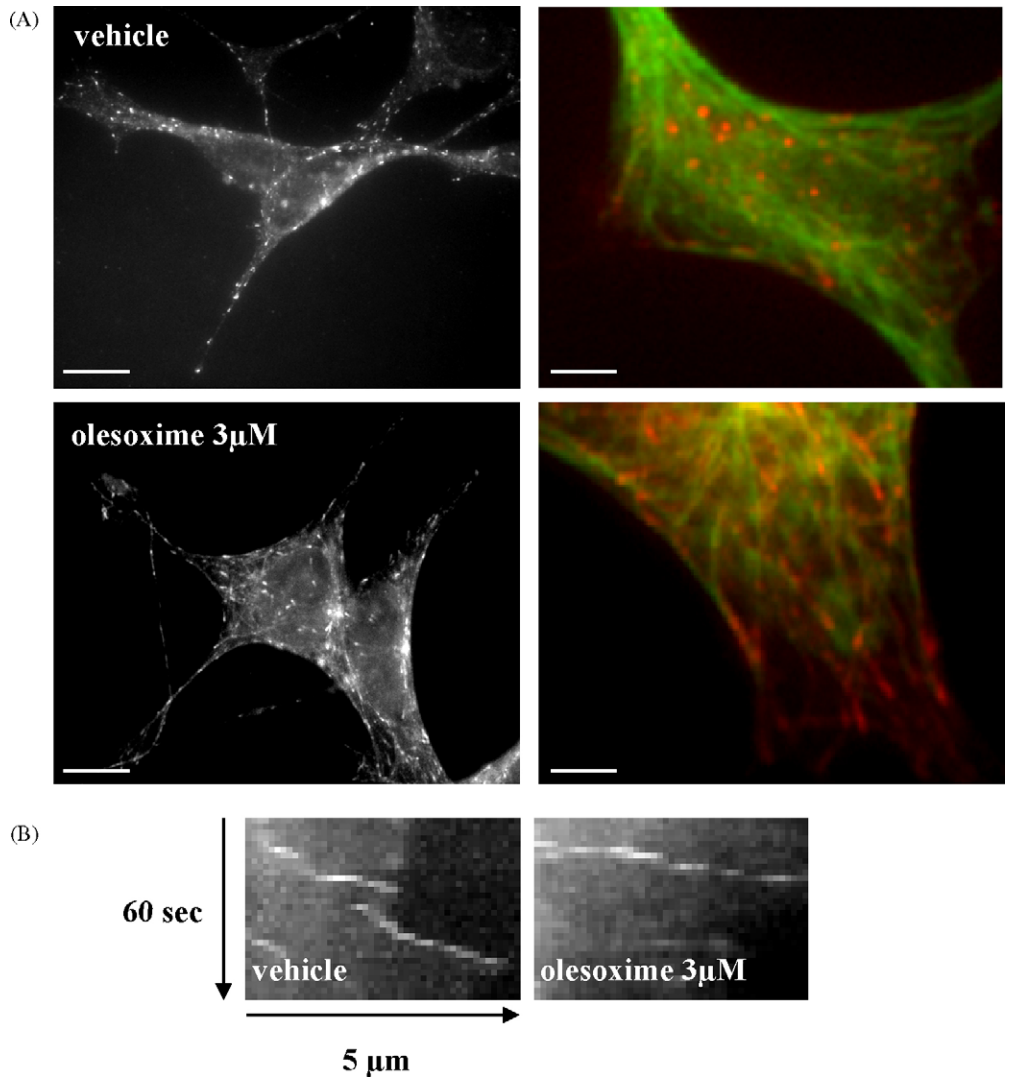

Fig. 3. Olesoxime enhanced EB1 accumulation and microtubule plus-ends dynamics in neuronal cells. (A) EB1 staining in differentiated SK-N-SH cells exposed for 6 h to vehicle or 3 μM olesoxime. Left photos show EB1 staining (scale bars: 20 μm), while the right ones are magnifications showing EB1 (red) and microtubule (green) co-staining (scale bars: 5 μm). (B) Visualization of EB1-GFP comet dynamics by kymographs in vehicle (left) and 3 μM olesoxime-treated (right) differentiated PC-12 cells. Comet velocity at plus-ends of growing microtubules was obtained by determining the slope of the line. (For interpretation of the references to color in this figure legend, the reader is referred to the web version of the article.)

confirming that neuroprotection was correlated with maintenance of microtubule plus-ends proteins.

3.5. Olesoxime did not prevent MTA-induced EB comet disruption in proliferating tumor and endothelial cells

Previous observations strongly suggest that the protective effects of olesoxime against MTA toxicity are specific to differentiated neuronal cells. To better assess this hypothesis, we examined the effects of MTAs combined with olesoxime on EB1 localization in proliferating SK-N-SH cells. In these cancer cells, 50 nM vincristine and 50 nM paclitaxel also triggered EB1 delocalization from microtubule plus-ends to cytosol after 6 h of treatment (Fig. 5A). In sharp contrast with results in differentiated SK-N-SH cells, concomitant treatment with olesoxime in proliferating SK-N-SH cells did not reverse the effects of MTAs on EB1 comet-like accumulation, since the fluorescence staining

Table 2
Olesoxime selectively increased the mean EB1 comet length (μm) in differentiated neuronal cells.

Cell lines	Vehicle	Olesoxime 3 μM
Differentiated SK-N-SH	0.64 ± 0.02	0.85 ± 0.02**
SK-N-SH	0.86 ± 0.04	0.82 ± 0.03 NS
U 87	1.01 ± 0.03	0.95 ± 0.03 NS
HUVEC	1.54 ± 0.04	1.52 ± 0.03 NS

NS, $p > 0.05$ (Student's *t*-test).
**$p < 0.01$ (Student's *t*-test).

Table 3
Olesoxime increased microtubule dynamics in growth cones of differentiated neuronal cells. Measurement of microtubule dynamics parameters by videomicroscopy of EB1-GFP at microtubule plus-ends in differentiated PC-12 cells exposed to vehicle or 3 μM olesoxime for 24 h.

Variables	Vehicle	Olesoxime 3 μM	Olesoxime *vs* vehicle
Growth rate (μm/min)	13.9 ± 0.7	16.6 ± 0.8*	+20%
% of time growing	92.3 ± 0.5	96.4 ± 1.9**	+4%
% of time pausing	7.7 ± 0.5	3.6 ± 1.9**	−54%

* $p < 0.05$ (Student's *t*-test).
** $p < 0.001$ (Student's *t*-test).

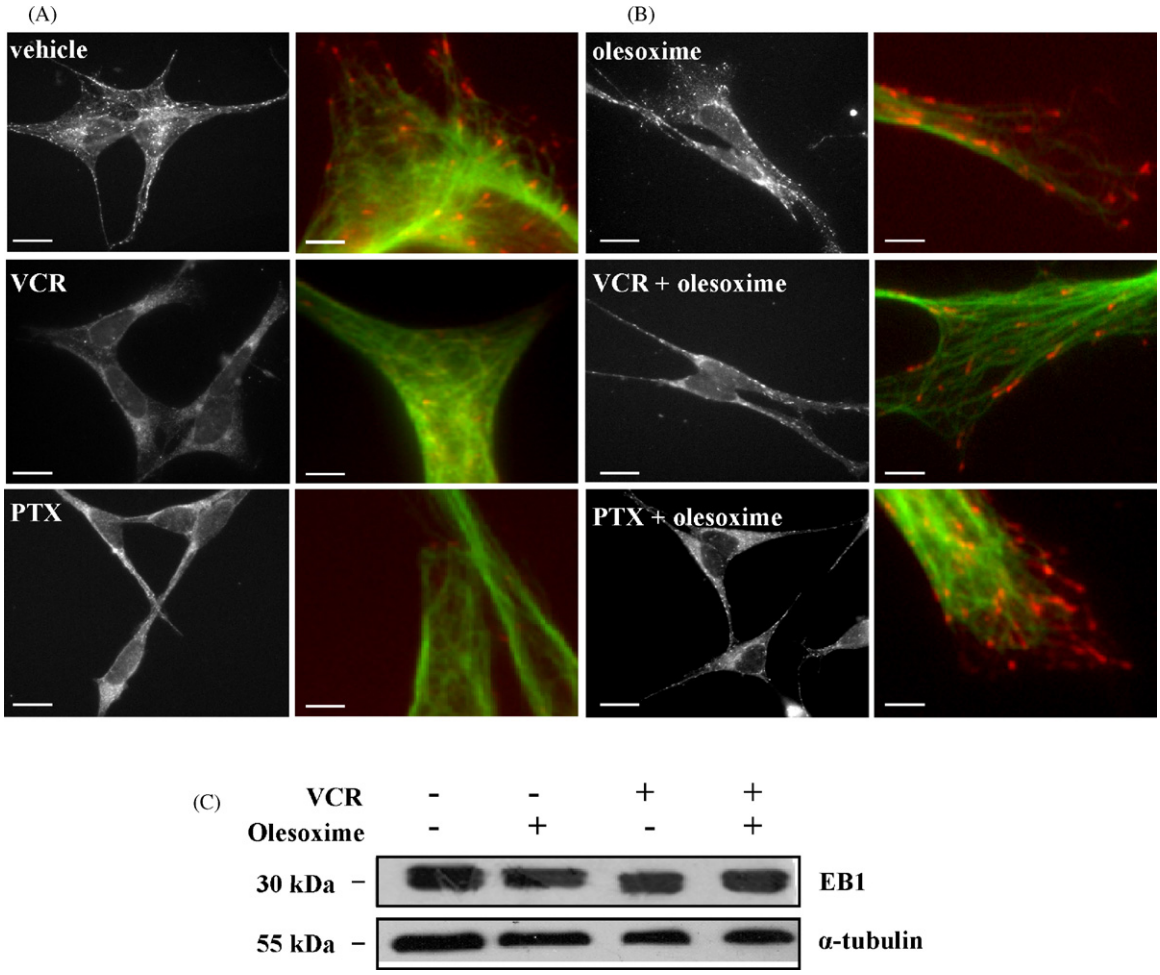

Fig. 4. Preservation of EB1 comets at microtubule plus-ends was associated with neuroprotection. EB1 staining in differentiated SK-N-SH cells exposed for 6 h to (A) vehicle, 100 nM vincristine (VCR), 50 nM paclitaxel (PTX), (B) 3 μM olesoxime alone or in combination with MTAs. Left photos show EB1 staining (scale bars: 20 μm), while the right ones are magnifications of EB1 (red)/microtubule (green) co-staining (scale bars: 5 μm). (C) Western blot analysis of EB1 expression in differentiated SK-N-SH cells treated with vehicle, 3 μM olesoxime, 100 nM vincristine treated or the combination of olesoxime and vincristine. Western blot analysis of total α-tubulin in each sample was used as a loading control. (For interpretation of the references to color in this figure legend, the reader is referred to the web version of the article.)

remained diffuse (Fig. 5A). Similarly, alteration of EB1 comet distribution in primary human endothelial cells treated for 24 h with 5 nM vincristine was not inhibited by olesoxime (Fig. 5B). Thus, olesoxime's ability to maintain microtubule plus-ends localization of EB1 was only observed in differentiated neuron-like cells.

3.6. Olesoxime restored mitochondrial motility in MTA-treated neuron-like cells

Since microtubules are structural tracks for the anchoring and transport of mitochondria, we studied modifications in mitochondrial movements in neurotoxic and neuroprotective conditions as a marker of microtubule functions (Fig. 6A; movies 2 and 3). By live imaging fluorescence microscopy of differentiated SK-N-SH cells, we showed that mitochondria mean velocity significantly decreased from 0.073 ± 0.006 μm/s in control cells to 0.018 ± 0.003 μm/s in cells treated with 100 nM vincristine (−75%) (Fig. 6B). Co-treatment with 3 μM olesoxime protected cells from vincristine-induced mitochondrial transport suppression, since organelle velocity was restored by 64% and reached 0.050 ± 0.006 μm/s ($p < 0.05$). Thus, olesoxime is likely to prevent MTA-mediated disturbance in microtubule dynamics and functions, including perturbation of the mitochondrial trafficking in neuronal cells.

4. Discussion

Prevention or even treatment of neuropathies associated with the clinical use of MTAs is a major medical need. Here, we evaluated olesoxime's neuroprotective properties in rat differentiated PC-12 cells, a widely used model to investigate CIPN [30], as well as in human differentiated SK-N-SH cells, a model biochemically, ultrastructurally and electrophysiologically comparable to human sympathetic neurons [31]. We showed that olesoxime was highly effective in preventing both paclitaxel- and vincristine-induced neurotoxicity in these two neuronal cell lines, in agreement with its previously reported beneficial effects in animal models of MTA-induced peripheral neuropathy [19,20]. Importantly neuroprotective activities of olesoxime correlated with the enrichment of microtubule plus-ends with EB proteins and the promotion of microtubule dynamics in neuronal cells. In addition, we demonstrated that olesoxime did not interfere with the anti-mitotic and the cytotoxic activity of either taxanes or Vinca alkaloids for several human tumor cell lines (i.e. neuroblastoma, lung and breast cancers). Altogether, our data strongly support the potential benefit of olesoxime to be used in combination with MTAs to prevent CIPN a significant unmet medical need.

While usually divided into two distinct classes, either as stabilizing or depolymerizing microtubule agents respectively, taxanes and Vinca alkaloids were shown to modulate dynamics of

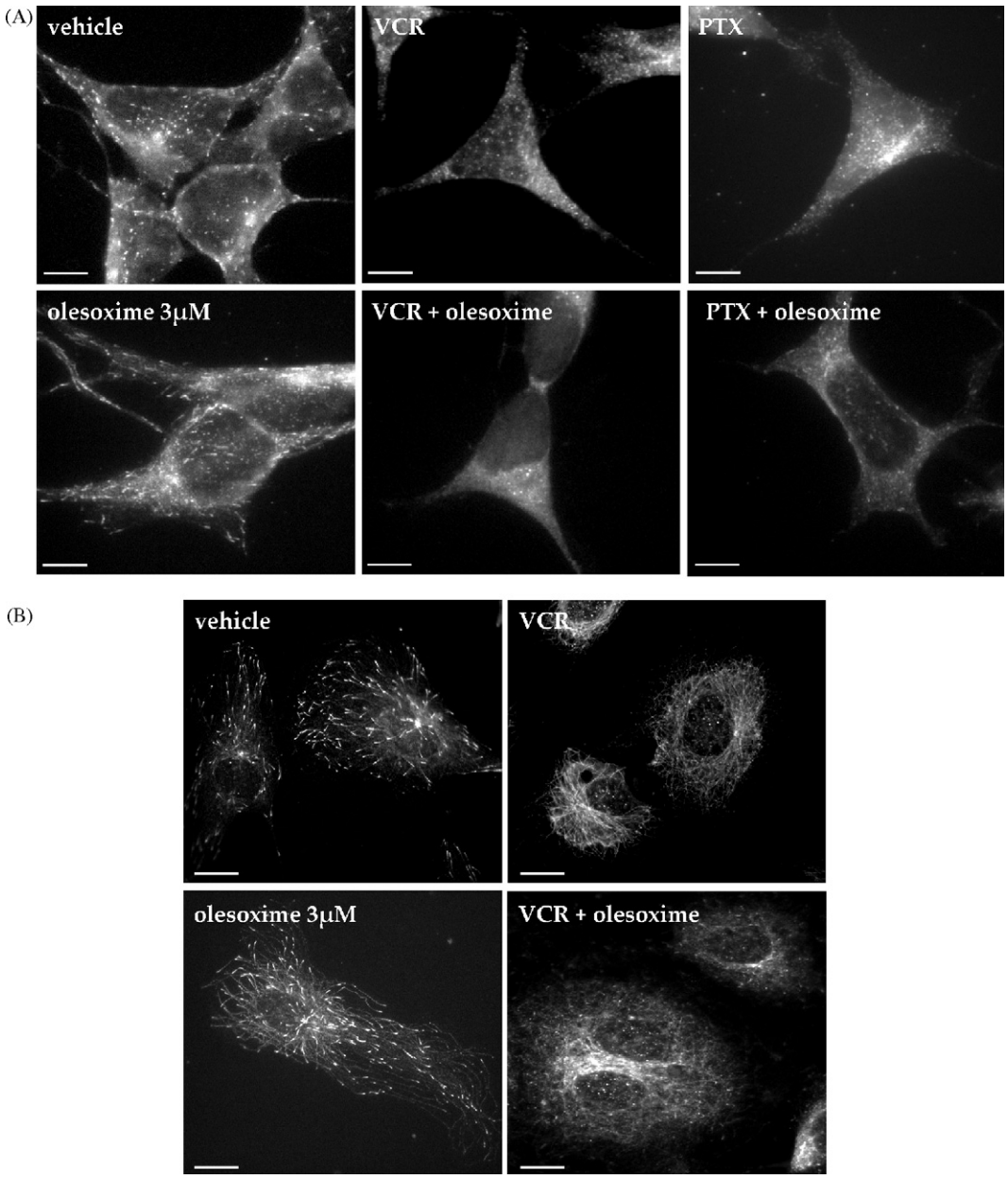

Fig. 5. Olesoxime did not prevent EB1 comet disruption in proliferating neuroblastoma or endothelial cells. (A) EB1 staining in undifferentiated proliferating SK-N-SH tumor cells exposed for 6 h to 50 nM vincristine (VCR), 50 nM paclitaxel (PTX), 3 μM olesoxime or olesoxime in combination with MTAs (scale bars 15 μm). (B) EB1 staining in HUVEC exposed for 24 h to 5 nM vincristine, 3 μM olesoxime or their combination (scale bars 25 μm).

microtubule plus-ends [32,33] and disrupt EB protein distribution in tumor cells [28,29,34,35]. Only recently, it was suggested that their neurotoxicity could arise from impaired microtubule dynamics, affecting neurite outgrowth. Indeed, neurotoxic concentrations of paclitaxel were associated with a decreased number and length of EB3 comet tails in neurons, suggestive of an association between the loss of EB proteins and reduced rate of microtubule growth or shortening [16]. The results presented here further support this hypothesis as the neurotoxic side-effects of both paclitaxel and vincristine were correlated with the suppression of EB1 and EB3 comet accumulation at microtubule plus-ends in differentiated neuronal cells. Thus, restoring EB protein localization using olesoxime might prevent MTA-induced neurite retraction. To our knowledge, olesoxime is the first described molecule that promotes EB protein accumulation at microtubule plus-ends. Previous studies of MTA-induced neuropathy in rats suggested that mitochondrial toxicity plays a role in CIPN and that drugs that improve mitochondrial dysfunction such as acetyl-L-carnitine (ALC) or olesoxime may be beneficial [8,10,18,19]. Interestingly, although reducing paclitaxel-induced pain and nerve fiber hyperexcitability, ALC did not prevent intraepidermal nerve fiber degeneration in paclitaxel-treated rats [36] while olesoxime does [20]. This suggests that olesoxime may have additional effects pertinent to MTA-induced CIPN and identifies EB proteins as new potential target(s) for neuroprotection. Accordingly, ALC was not able to restore EB1 at microtubule plus-ends in MTA-treated neuron-like cells (unpublished personal data), in sharp contrast with olesoxime.

Recent in vitro studies have allowed the understanding of the molecular mechanism of +TIPs localization at microtubule plus-ends based on a structural difference between the microtubule plus-end and the lattice [13,37]. However, very little is known about MTA action on +TIPs. Tubulin and microtubule conformational changes induced by taxanes and Vinca alkaloids may alter

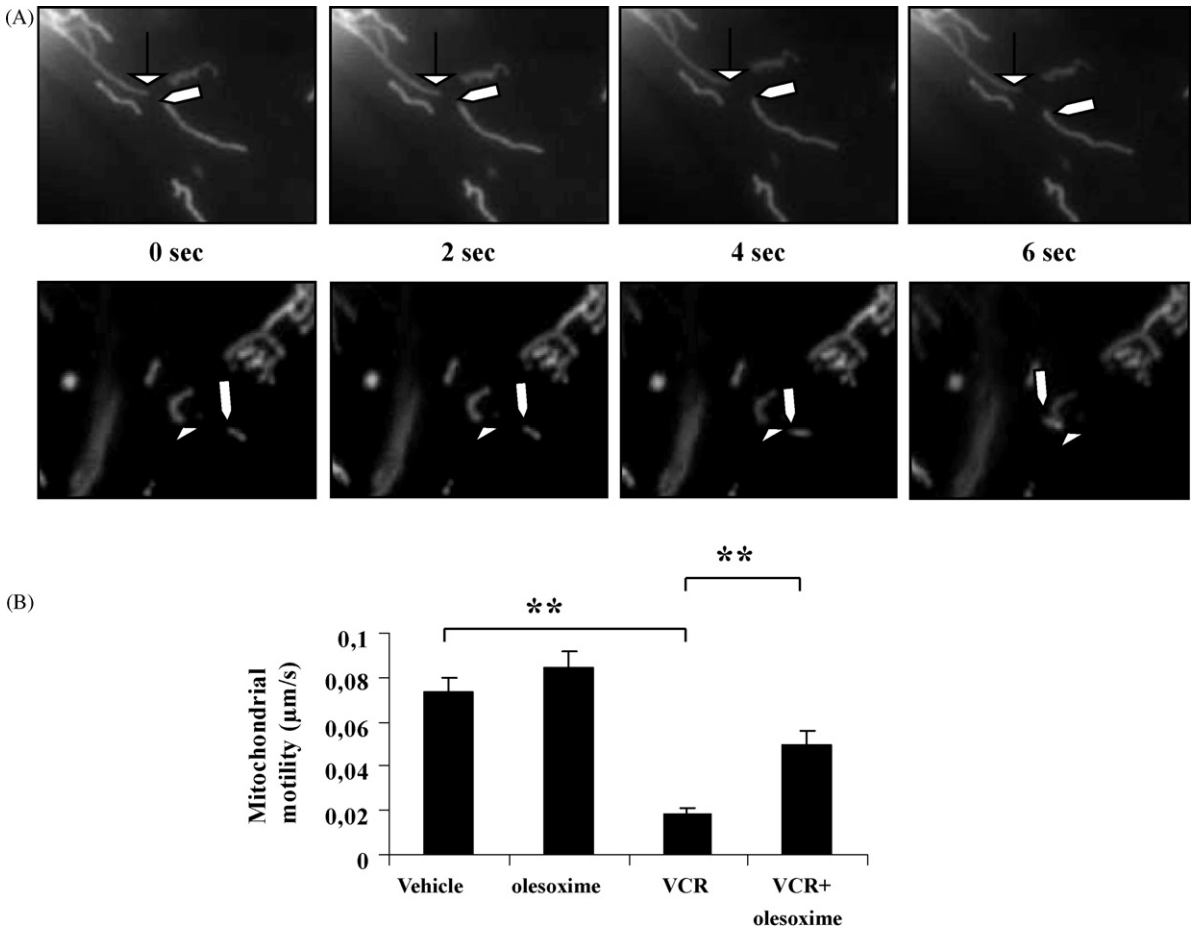

Fig. 6. Olesoxime prevented MTA-suppressed mitochondria motility. (A) Examples of mitochondria position tracks; arrow heads show two different movements of tubular (upper panel) or individual (lower panel) mitochondria. (B) Mitochondrial motility measurement in differentiated SK-N-SH cells exposed for 24 h to 3 μM olesoxime, 100 nM vincristine (VCR) and their combination (**$p < 0.01$; Student's *t*-test).

+TIPs-tubulin interaction or decrease the available EB binding sites at microtubule plus-ends. In support of this hypothesis, in vitro studies have shown that nocodazole modifies microtubule plus-end conformation [38]. In contrast, olesoxime may induce changes in the conformation of microtubule plus-ends in a manner that increases the number of binding sites available for EB proteins. Alternatively, MTAs could regulate EB-microtubule interaction via specific changes on EB protein phosphorylation [13], which could be prevented by olesoxime. Whatever the molecular mechanism(s) involved, MTAs by depleting EB proteins from microtubules are likely to result in loss of their anti-catastrophe activity and subsequent microtubule shortening. Reversion of this process might be thus responsible for olesoxime protection of both neurite shrinkage in vitro and loss of nerve endings in vivo. In addition, we showed that microtubule-governed mitochondria motility was blocked by MTAs and restored when combined with olesoxime. Since MTAs are able to directly target mitochondria [39–42], whether their effects on microtubule and mitochondria networks are separate or dependent is still an unsolved issue. Similarly, olesoxime binds to the mitochondrial proteins TSPO and VDAC [18]. Since tubulin associates with VDAC in the mitochondrial outer membrane [43,44], we can speculate that olesoxime may also counteract MTA-induced mitochondrial dysfunction by inhibiting their binding to the tubulin-VDAC complex.

The neuronal-specific mechanism of action of olesoxime is of major interest for a potential therapeutic to treat cancer patients. Indeed, olesoxime had no effect on MTA-disrupted EB1 binding to microtubule plus-ends in proliferating neuroblastoma cells, consistent with its lack of effect on MTA anticancer efficacy for a range of human tumor cell types. Similarly, olesoxime did not protect endothelial cells from EB1 comet displacement induced by MTAs, suggesting that MTA anti-angiogenic activity might also be preserved. We cannot exclude that olesoxime's neuronal selective effects on EB-microtubule interaction may be due to particular features of the neuronal microtubule network itself, such as neuron-specific tubulin isotypes or post-translational modifications [45,46]. Olesoxime may also modify microtubule assembly, via an effect on microtubule-associated proteins. Indeed, olesoxime is a cholesterol-like molecule [18], and cholesterol deficiency was shown to induce selective inhibition of MAP2 phosphorylation during neurite retraction [47]. In addition, cholesterol-like molecules such as neurosteroids bind to MAP2 and stimulate the polymerization of microtubules, preventing nocodazole-induced retraction of neurites in cultures [47,48]. Importantly, MAP2 is implicated in regulating microtubule organization and dynamics during neuronal polarization [45]. Involvement of such a microtubule-associated protein, neuron-specific tubulin isoforms or post-translational modifications in olesoxime's mechanism of action requires further investigation but could, at least in part, explain its selective neuronal activity.

In addition to its ability to prevent MTA-induced neurodegeneration [18,19], olesoxime promotes neurite outgrowth in primary motor neuron cultures and increases nerve regeneration after peripheral nerve lesion [19]. These results suggested that, beyond its neuroprotective properties, olesoxime displayed regenerative activities making this drug an ideal candidate for treatment of

neurodegenerative diseases, for example motor neuron disorders. Here, we demonstrate that olesoxime enhances EB protein accumulation at microtubule plus-ends in differentiated neuronal cells and increases microtubule growing events in growth cones. Such effects could explain how olesoxime promotes neurite outgrowth in primary neuronal cultures though this remains to be further explored. Interestingly, olesoxime's neuroprotective effects were associated with restored mitochondrial transport. Axonal and especially mitochondrial transport defects are common features of many neurodegenerative disorders, including amyotrophic lateral sclerosis, Huntington's disease or Alzheimer's disease (recently reviewed in [49,50]). In many of these diseases, disruption of axonal transport is an early event leading to altered functions of cargoes. Inversely, mitochondrial dysfunction is likely to affect axonal transport by a decrease in ATP supply to molecular motors. Results presented here reinforce the idea that olesoxime may be of interest for treatment of such defects, restoring microtubule dynamics and active mitochondrial axonal transport.

To conclude, we demonstrated here that the common neurotoxicity of taxanes and Vinca alkaloids correlates with the disturbance of both microtubule dynamics and microtubule-governed mitochondria trafficking in neuronal cells. By contrast, olesoxime's actions to preserve functions of the cytoskeleton and the mitochondrial network may contribute to its ability to prevent MTA-induced neurotoxicity. Olesoxime thus appears to be a promising drug candidate to treat CIPN but also other neurodegenerative disorders where microtubule-associated axonal transport is defective.

Acknowledgements

We thank Stéphane Honoré for helpful comments on the manuscript, Nathalie McKay for technical assistance and Romain Guilhaumou for determination of vincristine intracellular concentration. We also thank Maxime Lehmann and Hervé Kovacic for crucial help in fluorescence microscopy. This work was partly supported by the Cancéropôle PACA, INCa (France), and by the European Community under the 7th Framework Programme for RTD - Project MitoTarget - Grant Agreement HEALTH-F2-2008-223388. AR received a fellowship from the Région Provence Alpes Côte d'Azur (France).

Appendix A. Supplementary data

Supplementary data associated with this article can be found, in the online version, at doi:10.1016/j.bcp.2010.04.018.

References

[1] Argyriou AA, Koltzenburg M, Panagiotis P, Papapetropoulos S, Kalofonos HP. Peripheral nerve damage associated with administration of taxanes in patients with cancer. Crit Rev Oncol/Hematol 2008;66:218–28.
[2] Wolf S, Barton D, Kottschade L, Grothey A, Loprinzi C. Chemotherapy-induced peripheral neuropathy: prevention and treatment strategies. Eur J Cancer 2008;44:1507–15.
[3] Sioka C, Kyritsis AP. Central and peripheral nervous system toxicity of common chemotherapeutic agents. Cancer Chemother Pharmacol 2009;63:761–7.
[4] Hausheer FH, Schilsky RL, Bain S, Berghorn EJ, Lieberman F. Diagnosis, management, and evaluation of chemotherapy-induced peripheral neuropathy. Semin Oncol 2006;33:15–49.
[5] Bordet T, Pruss RM. Targeting neuroprotection as an alternative approach to preventing and treating neuropathic pain. Neurotherapeutics 2009;6:648–62.
[6] Kaley J, DeAngelis L. Therapy of chemotherapy-induced peripheral neuropathy. Br J Haematol 2009;145:3–14.
[7] Polomano RC, Mannes AJ, Clark US, Bennett GJ. A painful peripheral neuropathy in the rat produced by the chemotherapeutic drug, paclitaxel. Pain 2001;94:293–304.
[8] Flatters SJ, Bennett GJ. Studies of peripheral sensory nerves in paclitaxel-induced painful peripheral neuropathy: evidence for mitochondrial dysfunction. Pain 2006;122:245–57.
[9] Siau C, Xiao W, Bennett GJ. Paclitaxel- and vincristine-evoked painful peripheral neuropathies: loss of epidermal innervation and activation of Langerhans cells. Exp Neurol 2006;201:507–14.
[10] Pisano C, Pratesi G, Laccabue D, Zunino F, Lo Giudice P, Bellucci A, et al. Paclitaxel and Cisplatin-induced neurotoxicity: a protective role of acetyl-L-carnitine. Clin Cancer Res 2003;9:5756–67.
[11] James SE, Burden H, Burgess R, Xie Y, Yang T, Massa SM, et al. Anti-cancer drug induced neurotoxicity and identification of Rho pathway signaling modulators as potential neuroprotectants. Neurotoxicology 2008;29:605–12.
[12] Gu J, Firestein BL, Zheng JQ. Microtubules in dendritic spine development. J Neurosci 2008;28:12120–4.
[13] Akhmanova A, Steinmetz MO. Tracking the ends: a dynamic protein network controls the fate of microtubule tips. Nat Rev Mol Cell Biol 2008;9:309–22.
[14] Morrison EE, Moncur PM, Askham JM. EB1 identifies sites of microtubule polymerisation during neurite development. Brain Res Mol Brain Res 2002;98:145–52.
[15] Temburni MK, Rosenberg MM, Pathak N, McConnell R, Jacob MH. Neuronal nicotinic synapse assembly requires the adenomatous polyposis coli tumor suppressor protein. J Neurosci 2004;24:6776–84.
[16] Shemesh OA, Spira ME. Paclitaxel induces axonal microtubules polar reconfiguration and impaired organelle transport: implications for the pathogenesis of paclitaxel-induced polyneuropathy. Acta Neuropathol 2010;119(2):235–48.
[17] Jaworski J, Hoogenraad CC, Akhmanova A. Microtubule plus-end tracking proteins in differentiated mammalian cells. Int J Biochem Cell Biol 2008;40:619–37.
[18] Bordet T, Buisson B, Michaud M, Drouot C, Galéa P, Delaage P, et al. Identification and characterization of cholest-4-en-3-one, oxime (Olesoxime), a novel drug candidate for amyotrophic lateral sclerosis. J Pharmacol Exp Ther 2007;322:709–20.
[19] Bordet T, Buisson B, Michaud M, Abitbol JL, Marchand F, Grist J, et al. Specific antinociceptive activity of cholest-4-en-3-one, oxime (TRO19622) in experimental models of painful diabetic and chemotherapy-induced neuropathy. J Pharmacol Exp Ther 2008;326(2):623–32.
[20] Xiao WH, Zheng FY, Bennett GJ, Bordet T, Pruss RM. Olesoxime (cholest-4-en-3-one, oxime): analgesic and neuroprotective effects in a rat model of painful peripheral neuropathy produced by the chemotherapeutic agent, paclitaxel. Pain 2009;147(1–3):202–9.
[21] Pourroy B, Carré M, Honoré S, Bourgarel-Rey V, Kruczynski A, Briand C, et al. Low concentrations of vinflunine induce apoptosis in human SK-N-SH neuroblastoma cells through a postmitotic G1 arrest and a mitochondrial pathway. Mol Pharmacol 2004;66:580–91.
[22] Pasquier E, Honoré S, Pourroy B, Jordan MA, Lehmann M, Briand C, et al. Antiangiogenic concentrations of paclitaxel induce an increase in microtubule dynamics in endothelial cells but not in cancer cells. Cancer Res 2005;65(6):2433–40.
[23] Bourgarel-Rey V, Savry A, Hua G, Carré M, Bressin C, Chacon C, et al. Transcriptional down-regulation of Bcl-2 by vinorelbine: identification of a novel binding site of p53 on Bcl-2 promoter. Biochem Pharmacol 2009;78(9):1148–56.
[24] Carré M, Carles G, André N, Douillard S, Ciccolini J, Briand C, et al. Involvement of microtubules and mitochondria in the antagonism of arsenic trioxide on paclitaxel-induced apoptosis. Biochem Pharmacol 2002;63(10):1831–42.
[25] Groninger E, Koopmans P, Kamps W, De Graaf S, Uges D. An automated HPLC method to determine intracellular vincristine concentrations in mononuclear cells of children with acute lymphoblastic leukaemia. Ther Drug Monitor 2003;25(4):441–6.
[26] Guilhaumou R, Solas C, Rome A, Giocanti M, Andre N, Lacarelle B. Validation of an electrospray ionization LC/MS/MS method for quantitative analysis of vincristine in human plasma samples. J Chromatogr 2010;878(3–4):423–7.
[27] Geraldo S, Khanzada UK, Parsons M, Chilton JK, Gordon-Weeks PR. Targeting of the F-actin-binding protein drebrin by the microtubule plus-tip protein EB3 is required for neuritogenesis. Nat Cell Biol 2008;10(10):1181–9.
[28] Stepanova T, Slemmer J, Hoogenraad CC, Lansbergen G, Dortland B, De Zeeuw CI, et al. Visualization of microtubule growth in cultured neurons via the use of EB3-GFP (end-binding protein 3-green fluorescent protein). J Neurosci 2003;23(7):2655–64.
[29] Honoré S, Pagano A, Gauthier G, Bourgarel-Rey V, Verdier-Pinard P, Civiletti K, et al. Antiangiogenic vinflunine affects EB1 localization and microtubule targeting to adhesion sites. Mol Cancer Ther 2008;7:2080–9.
[30] Geldof AA, Minneboo A, Heimans JJ. Vinca-alkaloid neurotoxicity measured using an in vitro model. J Neurooncol 1998;37:109–13.
[31] Ciccarone V, Spengler BA, Meyers MB, Biedler JL, Ross RA. Phenotypic diversification in human neuroblastoma cells: expression of distinct neural crest lineages. Cancer Res 1989;49:219–25.
[32] Jordan MA, Kamath K. How do microtubule-targeted drugs work? An overview. Curr Cancer Drug Targets 2007;7:730–42.
[33] Pasquier E, Honoré S, Braguer D. Microtubule-targeting agents in angiogenesis: where do we stand? Drug Resist Updat 2006;9:74–86.
[34] Ma Y, Shakiryanova D, Vardya I, Popov SV. Quantitative analysis of microtubule transport in growing nerve processes. Curr Biol 2004;14(8):725–30.
[35] Bu W, Su LK. Regulation of microtubule assembly by human EB1 family proteins. Oncogene 2001;20(25):3185–92.
[36] Xiao WH, Bennett GJ. Chemotherapy-evoked neuropathic pain: abnormal spontaneous discharge in A-fiber and C-fiber primary afferent neurons and its suppression by acetyl-L-carnitine. Pain 2008;135(3):262–70.

[37] Vitre B, Coquelle FM, Heichette C, Garnier C, Chrétien D, Arnal I. EB1 regulates microtubule dynamics and tubulin sheet closure in vitro. Nat Cell Biol 2008;10(4):415–21.
[38] Zovko S, Abrahams JP, Koster AJ, Galjart N, Mommaas AM. Microtubule plus-end conformations and dynamics in the periphery of interphase mouse fibroblasts. Mol Biol Cell 2008;19(7):3138–46.
[39] Estève MA, Carré M, Braguer D. Microtubules in apoptosis induction: are they necessary? Curr Cancer Drug Targets 2007;7:325–34.
[40] André N, Carré M, Brasseur G, Pourroy B, Kovacic H, Briand C, et al. Paclitaxel targets mitochondria upstream of caspase activation in intact human neuroblastoma cells. FEBS Lett 2002;532:256–60.
[41] Khawaja NR, Carré M, Pourroy B, Kovacic H, Braguer D. High potency of epothilones in neuroblastoma cells may involve mitochondria. In: American Association for Cancer Research (AACR) Meeting Abstracts, April. 2006. p. 118.
[42] André N, Braguer D, Brasseur G, Gonçalves A, Lemesle-Meunier D, Guise S, et al. Paclitaxel induces release of cytochrome c from mitochondria isolated from human neuroblastoma cells. Cancer Res 2000;60(19):5349–53.
[43] Rostovtseva TK, Sheldon KL, Hassanzadeh E, Monge C, Saks V, Bezrukov SM, et al. Tubulin binding blocks mitochondrial voltage-dependent anion channel and regulates respiration. Proc Natl Acad Sci 2008;105(48): 18746–51.
[44] Carré M, André N, Carles G, Borghi H, Brichese L, Briand C, et al. Tubulin is an inherent component of mitochondrial membranes that interacts with the voltage-dependent anion channel. J Biol Chem 2002;277(37):33664–9.
[45] Poulain FE, Sobel A. The microtubule network and neuronal morphogenesis: dynamic and coordinated orchestration through multiple players. Mol Cell Neurosci 2010;43(1):15–32.
[46] Hammond JW, Cai D, Verhey KJ. Tubulin modifications and their cellular functions. Curr Opin Cell Biol 2008;20(1):71–6.
[47] Fontaine-Lenoir V, Chambraud B, Fellous A, David S, Duchossoy Y, Baulieu EE, et al. Microtubule-associated protein 2 (MAP2) is a neurosteroid receptor. Proc Natl Acad Sci 2006;103(12):4711–6.
[48] Murakami K, Fellous A, Baulieu EE, Robel P. Pregnenolone binds to microtubule-associated protein 2 and stimulates microtubule assembly. Proc Natl Acad Sci 2000;97(7):3579–84.
[49] Chen H, Chan DC. Critical dependence of neurons on mitochondrial dynamics. Curr Opin Cell Biol 2006;18(4):453–9.
[50] De Vos KJ, Grierson AJ, Ackerley S, Miller CC. Role of axonal transport in neurodegenerative diseases. Annu Rev Neurosci 2008;31:151–73.